Progress In Electromagnetics Research M, Vol. 119, 89–103, 2023

Millimeter Wave Attenuation in the Coastal Area of the Gulf of Guinea Subject to Heavy Rainfalls

Benjamin Tanga Louk[1, *], Raphael Onguene[1], Serge R. Dzonde Naoussi[1], Sakaros Bogning[1], Jacques Etame[1], Modeste Kacou[2], and Patrick H. Ntanguen[3]

Abstract—Wireless communication systems have developed significantly over the last few decades. Due to the saturation of lower frequencies of microwave spectrum (3–30 GHz) and the increasing need for high speed, emerging systems for consumer or professional use are progressively shifting to upper microwave and millimeter waves. Our study proposes a methodology for evaluating and classifying losses on a vertically polarized millimeter wave link at 80 GHz. To achieve this, we simulated the link budget of a Nokia 80UBT millimeter wave link operating in its real propagation space (with overground) with Pathloss 5.1 Design tool. Then we built a 3.58 km full-scale link in the Tongo-Bassa watershed of the coastal city of Douala in Cameroon. Analysing data collected over the period from December 06, 2020 to December 16, 2021 under Power BI allowed us to characterize the response of the millimeter signal in free space, during dry and rainy seasons. We then challenge ITU-R P.837-7 and ITU-R.P.838-3 Recommendations on statistical models of rainfall for propagation modeling, especially for millimeter signals propagated in an equatorial climate with heavy rainfalls. The study estimated a rainfall rate for 0.01% of the time at 110.1 mm/h, with a millimeter link cut-off for a rainfall rate greater than 64.8 mm/h, with a specific attenuation due to rain of 6.5 dB/km.

1. INTRODUCTION

The research on wireless transmission systems, operating at frequencies from 60 to 90 GHz known as millimeter waves or E-band, remains limited due to lack of in-depth knowledge of the propagation channel [1]. Enhanced by the simplified regulatory approach chosen, unlicensed or low-cost access, the development of millimeter frequencies is very well established in continental regions where the weather regime is dominated by continental, oceanic, and Mediterranean climates (North America and Europe) [2]. A survey carried out by the equipment manufacturer Ericsson in June 2015 shows that the millimeter waves, which a few years ago were not used, are experiencing a considerable boom in the wireless transmission market, and now have a solid global footprint [3, 4]. The dominant climate in the oceanic islands of the Gulf of Guinea is generally equatorial oceanic. Mean temperatures at sea level are 26°C in January and 24°C in July but decrease with altitude. The year is divided into two main seasons, a rainy season and a dry season, which are determined by the inter-tropical convergence zone and the interaction between the monsoon winds from the south of the Atlantic Ocean and the dry harmattan winds from the north of the Sahara and the Atlantic Ocean. Monsoon winds blow from the south of the Atlantic Ocean and the dry harmattan winds from the north of the Sahara and the Atlantic Ocean. On Mount Cameroon and Bioko, we have two dry season periods, one short and one long. The shorter dry season runs from July to August, and the longer dry season runs from December

Received 12 July 2023, Accepted 1 September 2023, Scheduled 25 September 2023
* Corresponding author: Benjamin Tanga Louk (benjamintangalouk@yahoo.fr).
[1] Technology and Applied Sciences Laboratory (TASL), University Institute of Technology, University of Douala, Cameroon.
[2] Atmospheric Physics and Fluid Mechanics (AP-FML), University F'elix Houphouët-Boigny, Abidjan, Ivory Coast. [3] Research Unit Condensed Matter, Electronics and Signal Processing, Department of Physics, University of Dschang, Cameroon.

to March [5]. In equatorial climates subject to heavy rainfalls such as the Gulf of Guinea, millimeter waves applications are very few or not deployed. Nigeria and Kenya are the pioneers in the deployment of E-band technologies in Africa [4, 6–8]. Using 2D Video Distrometer Data in Malaysia in 2017, an estimate of millimeter wave attenuation due to rain at the 38 GHz frequency for both vertical and horizontal polarisations was made and compared with other fits from neighboring areas and showed that ITU-R Recommendation P.838-3 underestimates the rain-specific attenuation by 6–25% [9]. The rain attenuation predicted by the ITU-R model varies non-monotonically with percentage of time and rain [10]. New prediction models for short path-length links help to improve the design of terrestrial links operating at millimeter wave frequencies in equatorial regions [11]. Our study focuses on the very first vertically polarised 80 GHz link installed by the manufacturer NOKIA in an equatorial environment for telephony operator Orange Cameroon, using new modulators (80 UBT). In this context, it was necessary to evaluate the millimeter wave link budget and, subsequently, determine the trend that mostly affects the millimeter wave propagation using data sets from a single link. This is a contribution to the elaboration of prediction models, thus enabling more accurate design of millimeter waves in an equatorial environment and more specifically in a watershed of the Gulf of Guinea (Tongo Bassa in Douala City).

2. MATERIALS AND METHODS

2.1. Wave Propagation Principles

The propagation channel, described as the transformation between the emitted signal and received signal, is presented by Collonge as below [1]:

$$Received\ Signal = Transformation(emitted\ signal) + noise \tag{1}$$

A logarithmic model as suggested in [12], taking into consideration the gain and loss elements that influence the performance of the transmission channel is presented as follows [12]:

$$RSL = P_0 - L_{tx} + G_{tx} - FSL - MFM - RA - L_{rx} + G_{rx} - L_m \tag{2}$$

The variables in the logarithmic model are known as the link budget of the link to be designed. They are either obtained from equipment manufacturer (transmitter, receivers, antennas cables, and connectors) or modelled (free space loss, rain attenuation, and multipath fading loss). We describe them in Table 1.

Table 1. The link budget components

Variable	Description	Unit
RSL	Received signal level	dBm
P_0	Emitted power	dBm
L_{tx}	Transmitting connexion loss	dB
G_{tx}	Transmitting antenna gain	dBi
FSL	Free Space Loss	dB
MFM	Multipath Fading Loss	dB
RA	Rain Attenuation	dB
L_{rx}	Receving connexion loss	dB
G_{rx}	Receving antenna gain	dB
L_m	Miscellaneous losses	dB

In this research, effects of Multipath Fading Loss (MFL) have been minimized by installing the antennas in a line-of-sight configuration that is fully Fresnel ellipsoidal regardless of the operating band (traditional band or millimetre band). Furthermore, the sum of miscellaneous losses has been estimated to 1 dB as recommended by the Alcatel University (merged into NokiaEDU in 2016) and adopted by Orange Cameroon [13]. As a result, the main link budget variables to be simulated in the E band remain Free Space Loss and Rainfall Attenuation.

2.1.1. Free Space Loss

Free Space Loss represents the major part of the total signal attenuation. It depends on the frequency (f) and the distance between the two antennas (d) and is derived from the Frisks transmission formula below [12, 14]:

$$L_{FSL} = 92.45 + 20\log(f) + 20\log(d) \tag{3}$$

2.1.2. Rainfall Attenuation

In February 2021, Samad et al. classified existing terrestrial rain attenuation models into five categories based on the formulation of the rain attenuation model; these include the empirical, statistical, physical, fade slope, and optimization-based models [15]. The taxonomy of well-known and recently developed rain attenuation models used in this study is presented in Figure 1.

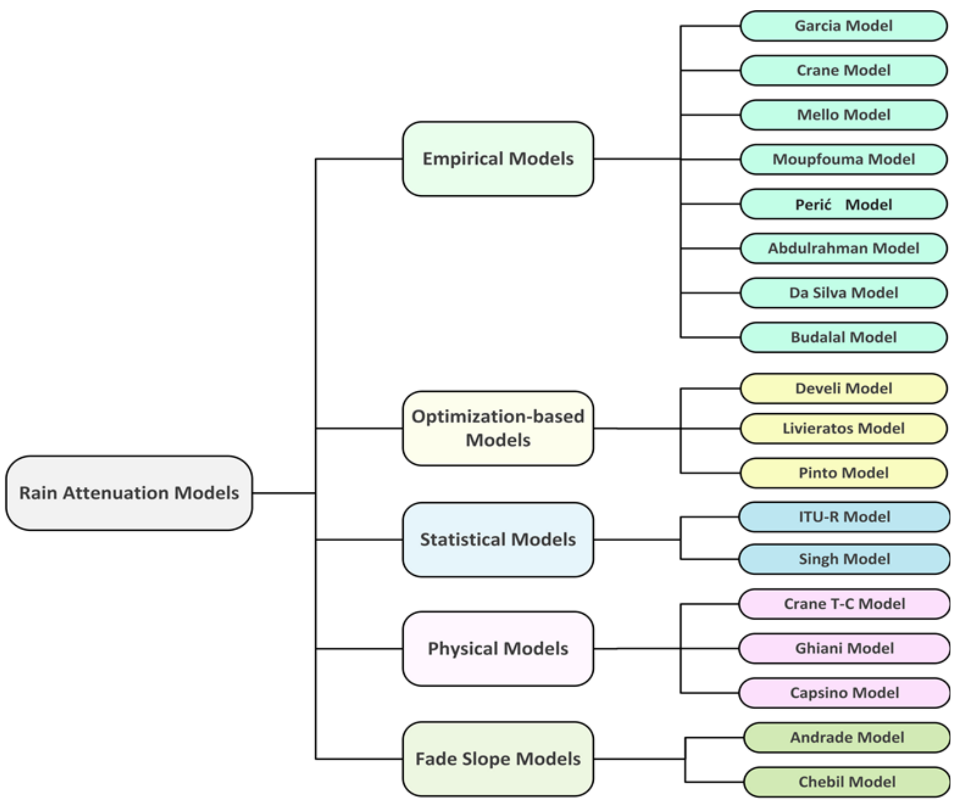

Figure 1. Taxonomy of terrestrial rain attenuation models.

Statistical models of rainfall attenuation were used in our analysis of millimetre wave attenuation in the equatorial area, especially ITU recommendations ITU-R. P.837-7 [16] and ITU-R.P.838-3 [17]. These recommendations were applied to design more than 2000 microwave links running with traditional band frequencies (11 GHz, 15 GHz, 18 GHz, and 23 GHz) for the backhaul transmission network of the operator Orange in Cameroon.

Millimetre wavelengths are of the order of magnitude of the raindrop size (millimetre) [12]. Thus, they interact with raindrops in a power-law relationship [9, 17]. Specific rain attenuation γ_R (dB/km) affecting the signal is correlated to the rain intensity R (mm/h) by Equation (4). The coefficients k and

α are experimentally obtained and mainly depend on operating frequency, wave polarization (Horizontal or Vertical), and raindrop size distribution [18]:

$$\gamma_R = kR^{\alpha} \tag{4}$$

The ITU-R P.837-7 recommendation addressing the topic of characteristics of precipitation for propagation modelling states that rainfall rate statistics with a 1 minute integration time are required for the prediction of rain attenuation in terrestrial links and Earth-space links [16].

Reliable long-term local precipitation rate data are available with integration times greater than 1 minute. Annex 2 to this recommendation provides a method for converting precipitation rate statistics with integration times greater than 1 minute into precipitation rate statistics with an integration time of 1 minute [16]. In our case, local rainfall rate data with integration time of 5 minutes is available. The recommended method is integrated in a computer program available in the Supplement. The software package used for this phase is CONVRRSTAT.ZIP, proposed by the Recommendation P-REC-P.837-7. The software has been developed under Matlab version R2009a and consists in a Graphical User Interface (GUI) [16]. Frequency-dependent coefficients k and α, for estimating specific rain attenuation using Equations (4), are given in Table 5 of Rec. ITU-R P.838-3 [17] for each polarization. Table 2 is an extract of the part that covers the frequencies and vertical polarization (V) used in our study.

Table 2. Extract of Table 5 of the Rec. ITU-R P.838-3: Frequency-dependent coefficients for estimating specific rain attenuation (Vertical polarization) [17].

Frequency (GHz)	k_V	α_V
71	1.0409	0.7193
72	1.0561	0.7171
81	1.1793	0.7004
82	1.1915	0.6988

For vertically polarized millimeter waves with Tx = 81875 MHz and Rx = 71875 MHz, the model estimates $k_{Tx} = 1.1915$, $\alpha_{Tx} = 0.6988$, $k_{Rx} = 1.0561$, and $\alpha_{Rx} = 0.7171$.

2.2. System Setup and Data Collection

2.2.1. Tongo-Bassa: Environmental Observatory

Located in one of the 13 catchment areas of the coastal city of Douala in Cameroon, the “Tongo-Bassa” environmental observatory served as a detection system for meteorological phenomena influencing the propagation of millimetre waves, mainly rainfall. The Tongo-Bassa watershed observatory consists of 18 measuring stations: 08 rain gauges, 07 hydrometers, 02 tide gauges, and 01 complete weather station consisting of an optical laser disdrometer known as the “Parsivel” (Figure 2(a)) [19–22]. Rainfall data from 04 tilting bucket rain gauges in particular, reference 15189 from the German manufacturer OTT Hydromet (Figure 2(b)), arranged around an 80 GHz test link were used to determine dry and rainy periods: “Météo-IUT”, “Campus-2-Université”, “Socatur”, and “Hôpital-Des-Soeurs”. The rainfall intensities are collected every 5 minutes and transmitted via an OTT netDL 500 modem (Figure 2(c)) to the central server of the Geosciences Environment laboratory in Toulouse and can be accessed on demand. More details on the equipment reliability can be consulted from the manufacture site https://www.otthydromet.com/en/(accessed on 28 March 2022). Rain gauges show good measurement reliability, as demonstrated by Ntanguen et al. [22], in their comparative study with the Parsivel disdrometer.

Table 3 gives details on geographical coordinates of the four rain gauges of the environmental observatory used in our study.

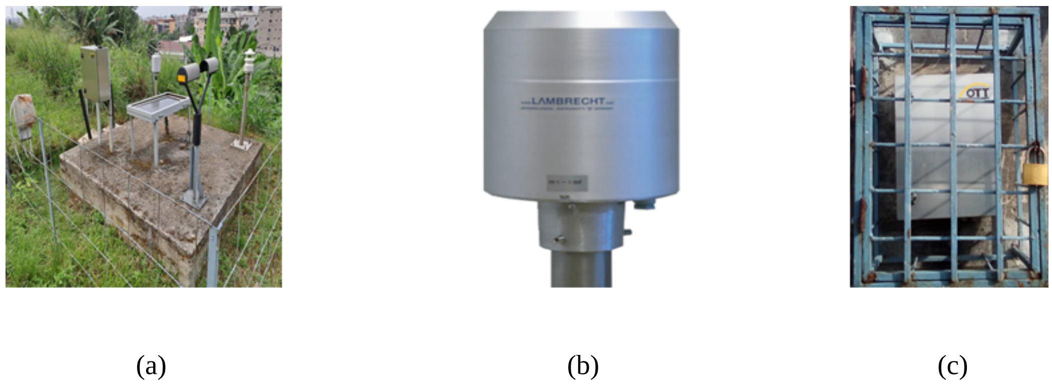

Figure 2. Acquisition and transmission stations of the environmental observatory of the Douala, Sustainable City: Sustainable development and valorization of the Makèpè Missokè site project in the Tongo-Bassa watershed. (a) Second generation OTT Parsivel disdrometer. (b) 15189 LAMBRECHT, Tilting bucket Rain gauges and (c) OTT netDL 500 modem for data transmition.

Table 3. Rain gauge locations in the Tongo-Bassa watershed.

Station Name	Latitude (N)	Longitude (E)
Météo-IUT	04°03′25.1″	009°44′42.7″
Campus-2-Université	04°03′23.5″	009°44′39.3″
Socatur	04°02′49.9″	009°44′43.7″
Hopital-Des-Soeurs	04°04′42.9″	009°46′04.3″

2.2.2. Carrier Aggregation (CA) Test Link

In order to study the attenuation of 80 GHz millimetre waves in the Tongo-Bassa catchment area in the city of Douala, we installed, within this area, an 80UBT-m radio link from Nokia vertically polarised test link. The four rain gauges of the observatory mentioned above are located all around the 3.58 km long test link. In parallel with this millimetre link, we built one 18 GHz traditional frequency band microwave link using Carrier Aggregation (CA) configuration. The purpose of this traditional link was for quality control of the installations and for analysis, interpretation, and assessment of the attenuation differences according to the frequency (80 GHz or 18 GHz). Thus, the CA test link is as summarised in the diagram in Figure 3.

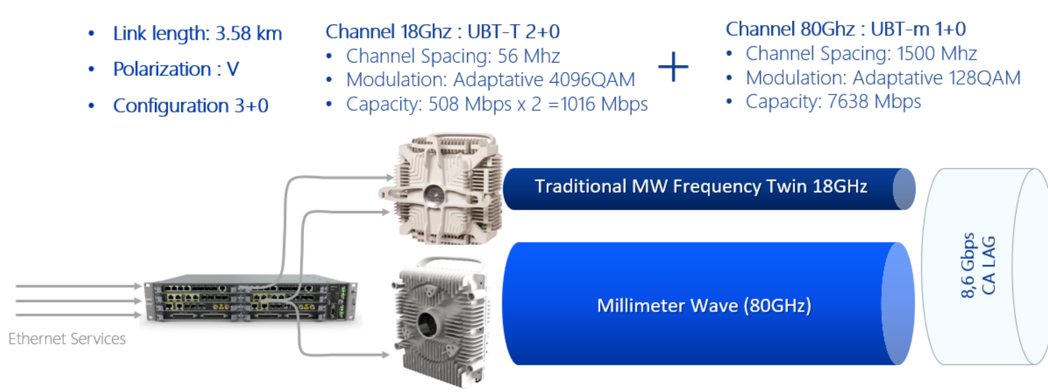

Figure 3. Carrier aggregation test link: millimeter waves (80 GHz) plus traditional wave (18 GHz).

The link design was based on the Pathloss V5.1 planning tool following the Alcatel University protocol [13, 23], whose conceptual order recommends the following steps: station geolocation; topology analysis; evaluation of free space losses and contribution from the ground; antenna sizing; evaluation of losses in cables, connectors, and other coupling modules; transceiver (ODU) design; frequency planning; and evaluation of rain attenuation. Table 4 contains the technical specifications of the test link installed between two points, Makepe and Ndogbong, located in the Tongo-Bassa catchment.

Table 4. Technical specifications of the millimeter wave test Link[2].

	Ndogbong	Makepe
Latitude	04 03 13.20 N	04 05 09.37 N
Longitude	009 45 03.30 E	009 45 10.60 E
Azimuth 3.61	183.61	
Elevation (m)	46.32	36.60
Antenna model	SC 2-W800B	SC 2-W800B
Antenna gain (dBi)	50.40	50.40
Antenna height (m)	39.40	34.00
Radio model	80UBT 1500 8129	80UBT 1500 8129
Frequency (MHz)	81875	71875
Polarization	Vertical	Vertical
Path length (km)	3.58	3.58
Tx Power (dBm)	6	6
Receive Power (dBm)	−39.11	−39.11

[2] The received power values calculated with the Pathloss V5.1 tool are symmetrical (equal) at the local and remote sites because of the frequency translation performed $F_{Central} = (\frac{F_{Min} - F_{Max}}{2})$.

We can therefore draw a mapping of millimetre wave attenuation measurement system in the coastal area of the Gulf of Guinea subject to heavy rainfall, particularly in the environmental observatory of the Tongo-Bassa catchment, Figure 4.

2.2.3. Data Collection

The Carrier Aggregation test link was integrated to Nokia's Network Services Platform, Network Functions Manager-Packet (NSP NFM-P). This monitoring platform collects transmitted and received power, frequency, modulation, capacity, and performance (unavailability, errored seconds, severely errored seconds and bit error rate) data of the studied link, every 15 minutes. Data were then saved and computed using NomadAutomate, which is a transport network OSS augmented by network intelligence functionality used as network management and optimization software. NomadAutomate is hosted into a 02 Terabytes capacity virtual server. The rainfall intensity data collected every 5 minutes and transmitted to the central server of the Douala City Council can be accessed at any time on a controlled request.

Thanks to this method, we collected, stored, processed, and analyzed data from the 80 GHz test link for one year: from 06th December 2020 to 16th December 2021. Given the large volume of data to be handled, deeper processing was done on Power BI Desktop.

2.3. Overall Methodology

In order to achieve the aim of this study, we carried out a number of steps, as shown in the general flowchart presented Figure 5: (1) field data acquisition and curation from site surveys including

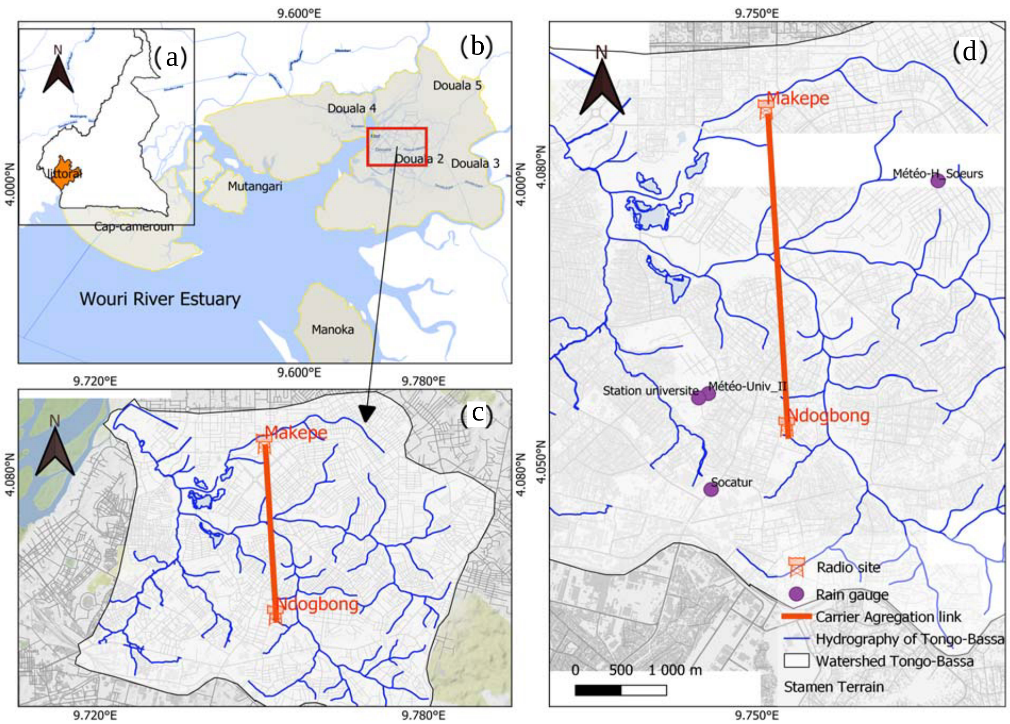

Figure 4. (a) Douala city on Cameroon map, located in in the coastal area of the Gulf of Guinea. (b) Wouri river estuary, tributaries, and surrounding districts. Douala subdivisions are presented in grey. (c) Location of the 80 GHz test link in Tongo Bassa catchment. Link installed between Makèpè and Ndogbong. (d) Presentation of the environmental observatory in Tongo-Bassa catchment. Focuss is made on the four Rain gauges sourrounding the 80 GHz test link.

topographic, land use, and over ground occupation, thus leading to the cartographic processing of study area, (2) millimeter wave link simulations and calibration, (3) full-scale link installation and monitoring, (4) one year data analysis. This was done with the aim of concluding on the relevance of using statistical models of ITU-R in the coastal area of the Gulf of Guinea.

3. RESULTS AND DISCUSSION

3.1. Characteristics of Precipitation

We combined the average rainfall intensities captured from the 4 rain gauges embedded in the study, during one full year, from the 06th December 2020 to the 16th December 2021. We obtained an annual distribution of rainfall in the Tongo-Bassa catchment area as illustrated in Figure 6.

The heaviest rainfall was recorded on 16th September 2021 between 03 : 10 AM and 03 : 20 AM. It reached the intensity of 140 mm/h. We also confirm that the driest period of the year occurred between December and February. Results in line are in agreement with those obtained by Tanessong et al. and by Findi et al. [24, 25].

3.2. Estimated Rain Rate Based on P-REC-P.837-7-CONVRRSTAT.ZIP Software

The conversion of our data recorded from 5 minutes to 1 minute, based on the P REC-P.837-7 standard, enabled us to obtain a rain rate of 110.1 mm/h for 0.01% of the time, as shown in Figure 7. The value of $R_{0.01}$ for 5 min is approximately 100 mm/h, with a deviation of 10.1 mm/h.

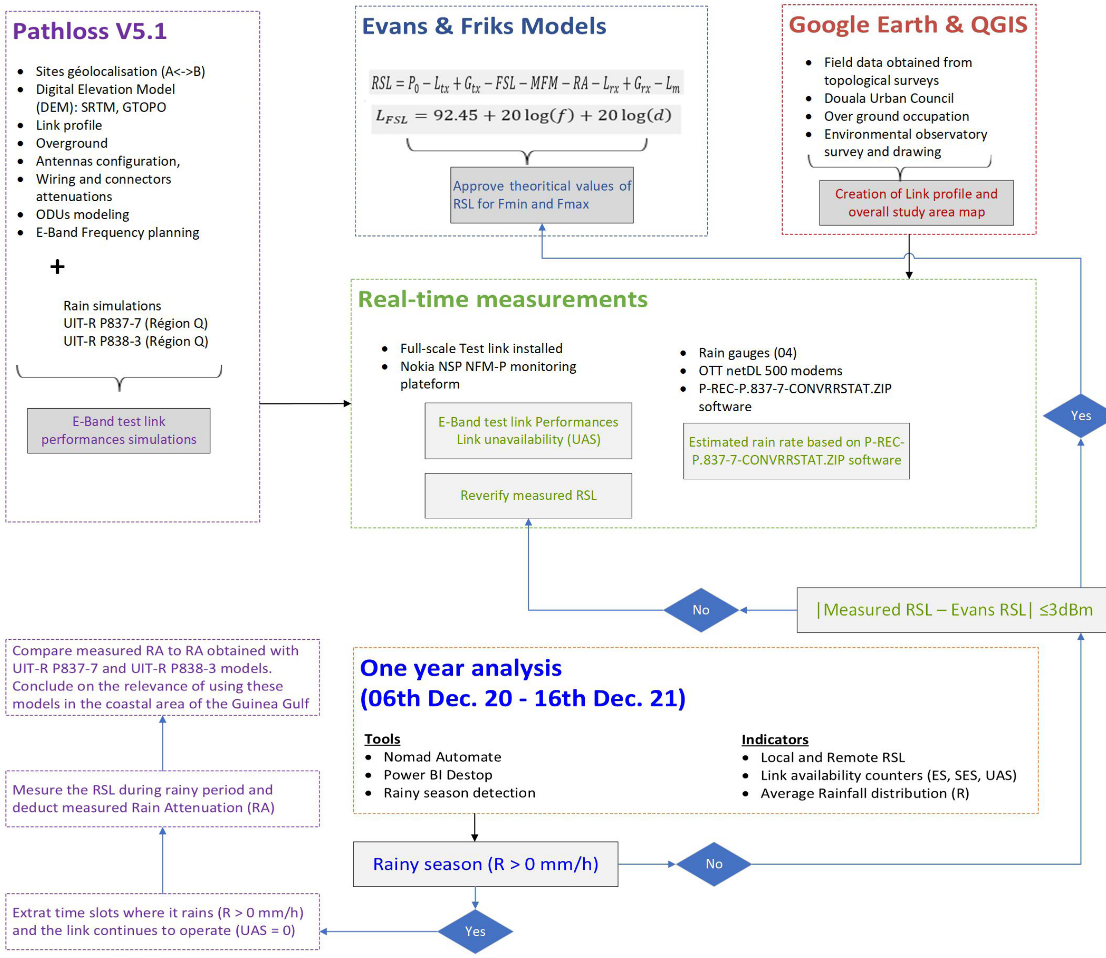

Figure 5. Overall methodology of the study.

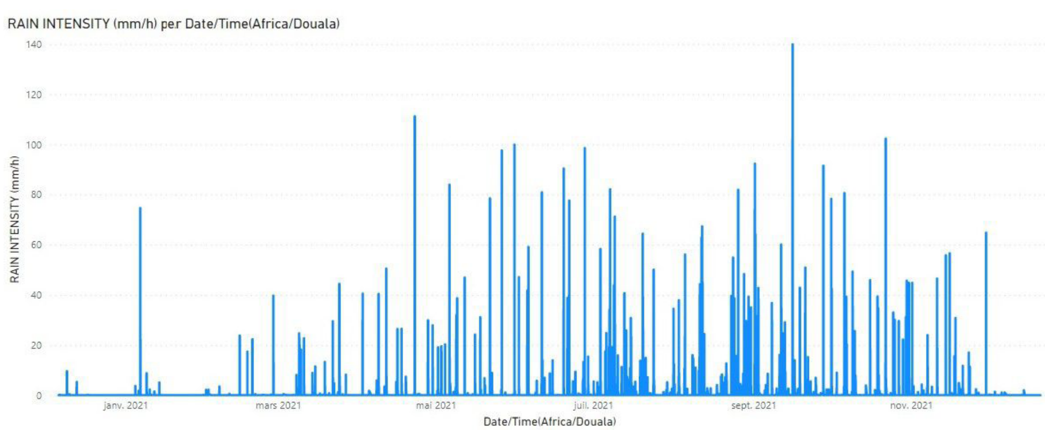

Figure 6. Measured Rainfall distribution in the Tongo-Bassa watershed from 06th December 2020 to 16th December 2021. Data captured from environmental observatory in Tongo-Bassa catchment.

3.3. Attenuation Analysis

A very strong correlation appears while superimposing the graphs of the RSL (Received Signal Levels in dBm), Link unavailability or interruption (in seconds) and Rainfall intensity (in mm/h) over the same

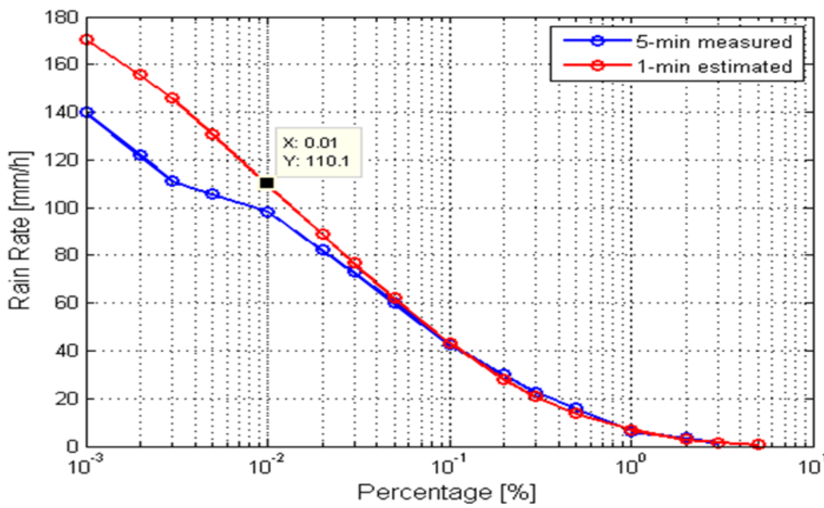

Figure 7. Estimated rain rate based on rain measurements from 06th December 2020 to 16th December 2021.

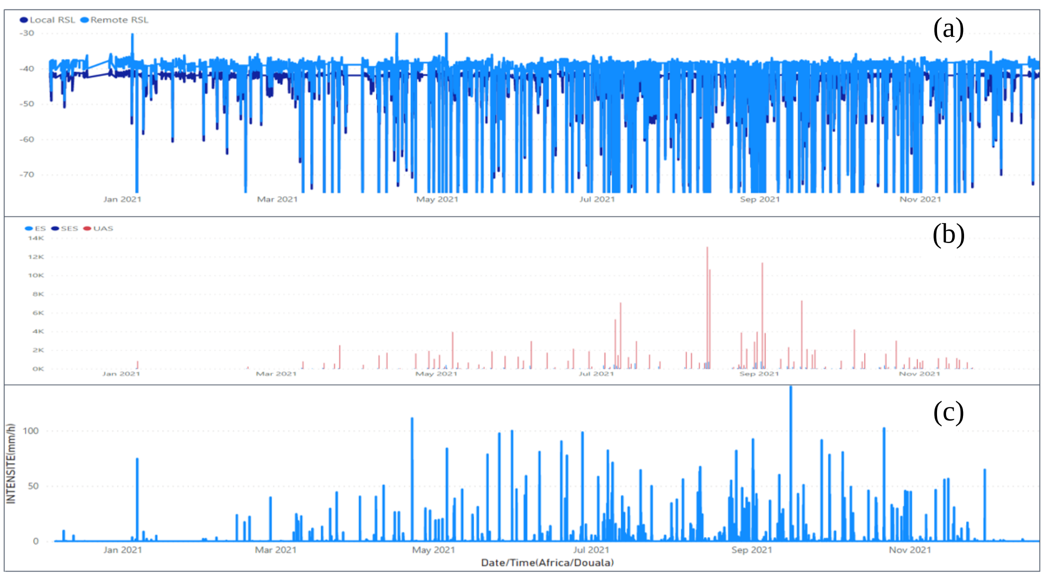

Figure 8. Annual correlation diagram. (a) Received Signal Level (RSL in dBm) in Local site (Makèpè) and Remote site (Ndogbong). The significant difference of more than 3 dB between the RSL values is explained by the 10 GHz duplex difference between the transmission frequencies in each site. (b) Link availability counters: ES = Errored Second, SES = Severely Errored Second and UAS = Unavailable Second. (c) Measured Rainfall distribution in the Tongo-Bassa watershed from 06th December 2020 to 16th December 2021.

observation window (06th December 2020-16th December 2021) (Figure 8). The 3.58 km long 80 GHz E-band test link installed is highly sensitive to rainfall. Performance counters show over 2000 seconds of downtime at rainfall intensities of 50 mm/h. During the period of heavy rainfall in September, more than 13,000 seconds of downtime were recorded, representing approximately 3.6 hours of test link outage. This leads us to analyse the 80 GHz test link in two periods: a dry season from December to February, and the rainy season from August to November.

3.3.1. Dry Season Attenuation

We consider as dry season the periods of the year when it did not rain at all. On the basis of this assumption, this period was defined from 06th December 2020 to 06th January 2021 (see Figure 9). During the dry season, the average received power at the local site (Ndogbong) receiving at high frequency (Fmax) is $-40.46\,\text{dBm}$. At the remote site (Makepe-Nodal) receiving at low frequency Fmin, the average received power value is $-38.24\,\text{dBm}$. We can synthesise the theoretical received millimetre signal power values, calculated with Pathloss 5.1 and determined from the graphs in Figure 10.

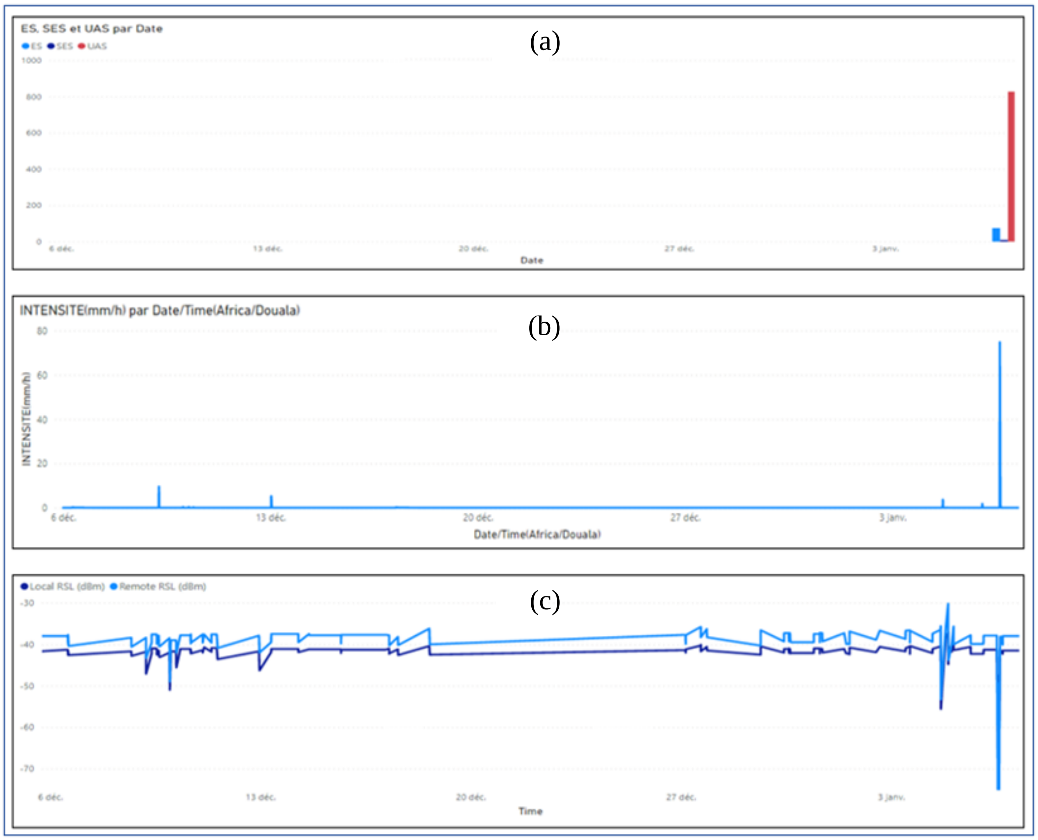

Figure 9. Dry season attenuation analysis. (a) Link availability counter shows no UAS meaning that the link was up and running during this period. (b) Measured Rainfall intensity. (c) RSL in local and remote sites.

Theoretical RSL values were obtained by combining Evans and Friks relations of Equations (2) and (3), respectively. Link budget components is provided by Nokia 80 UBT-m equipment datasheet.

During the dry season the difference between average theoretical RSL and the average measured RSL varies between $1.19\,\text{dB}$ and $2.28\,\text{dB}$ which are within the sizing margin of $\pm 3\,\text{dB}$ usually accepted by Orange Cameroon [13, 14] for microwave links. This confirms that the free space attenuation law Equation (3) remains valid for the $80\,\text{GHz}$ millimetre wave signal in the Gulf of Guinea region.

3.3.2. Rainy Season Attenuation

Depending on rainfall intensity, the millimeter test link may continue to operate when the reception threshold ($-74.1\,\text{dBm}$) is not reached, or it may shut down. In this study, we are interested in time slots where it rained (Rain Intensity $> 0\,\text{mm/h}$), and the test link continued to operate (UAS $= 0$). In the year 2021, these time slots were detected during the months of August, September, October, and November, as shown in Figure 11. Therefore, we have drawn up the summary diagram of Received

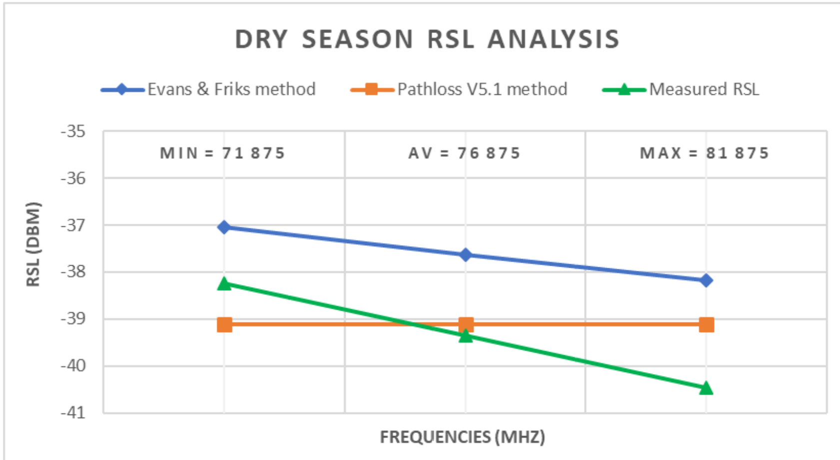

Figure 10. Dry season Received Signal Level (RSL) analysis.

Signal Level (RSL) analysis during the rainy season, presented in Figure 12. The observation of all other periods showed outages of the test link (non-zero UAS), despite the configured adaptive modulation function, making the analysis impossible. The minimum modulation of 1/4 BPSK for a capacity of 272 Mbps was not able to withstand rainfall intensities greater than 65 mm/h.

By subtracting dry season measured RSL from rainy season measured RSL, we deduce the contribution of the rain to the attenuation of the 80 GHz millimetre test signal, RA parameter in Equation (2). This allowed to construct a rain attenuation matrix for the millimetre signal (Table 5). Beyond these attenuation values, the link breaks down generating unavailable second (UAS).

Table 5. Rain Attenuation (RA) matrix for the 80 GHz millimetre test link.

Month	RA at Remote (dB)	RA at Local (dB)
August	25.34	26.86
September	14.44	15.26
October	32.84	34.06
November	19.94	21.56

As a reminder, the test link is 3.58 km long. We therefore deduce a linear average specific attenuation due to rainfall of: $\gamma_{Rmeasured} \Rightarrow 6.50$ dB/km. We have summarized the rainfall intensity and rain attenuation results in Table 6.

Table 6. Rainfall Intensity and Rain Attenuation analysis summary.

Indicator description	Value
Tx or local site Frequency (MHz)	81875
k	1.1915
α	0.6988
P-REC-P.837-7 estimated Rain Intensity R (mm/h)	110.10
Rec. ITU-R P.838-3 predicted specific RA (dBm/km)	31.83
Measured Rain Intensity before link cutoff (mm/h)	64,80
Measured specific RA (dBm/km)	66.50

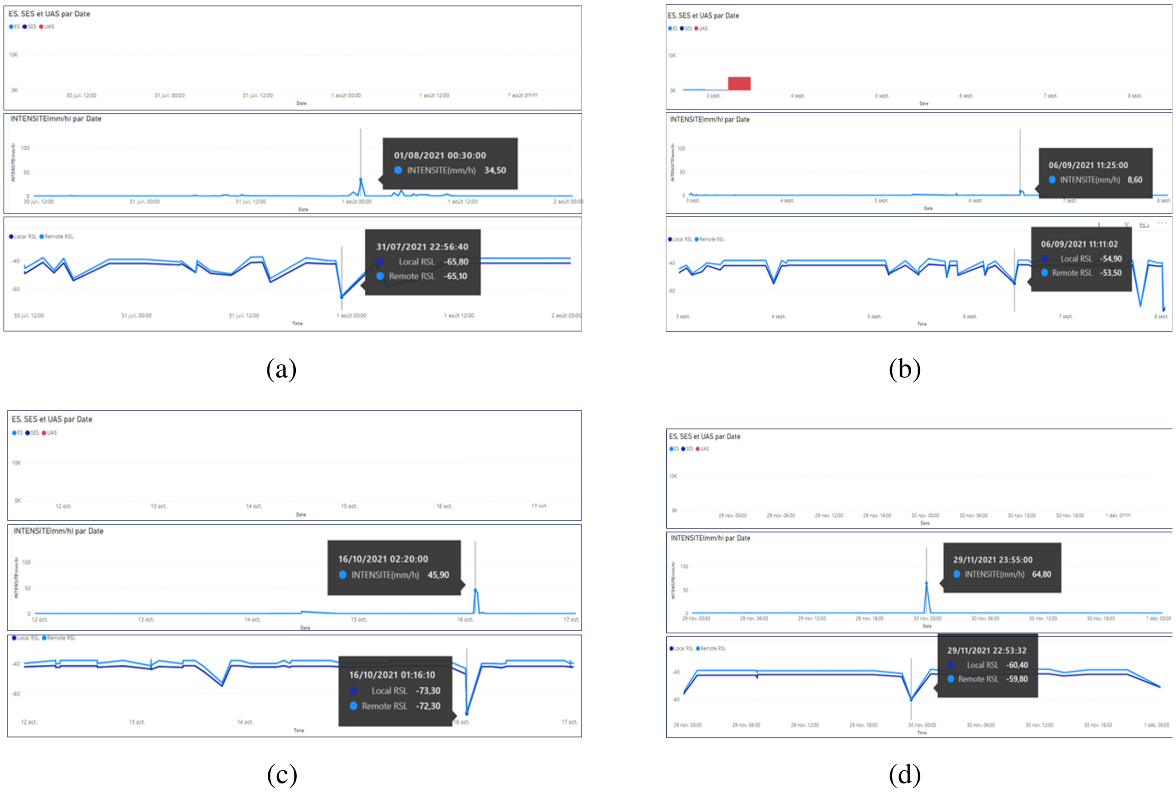

Figure 11. Measurement of RSL in the rainy season over the year 2021 (a) August, (b) September, (c) October and (d) November.

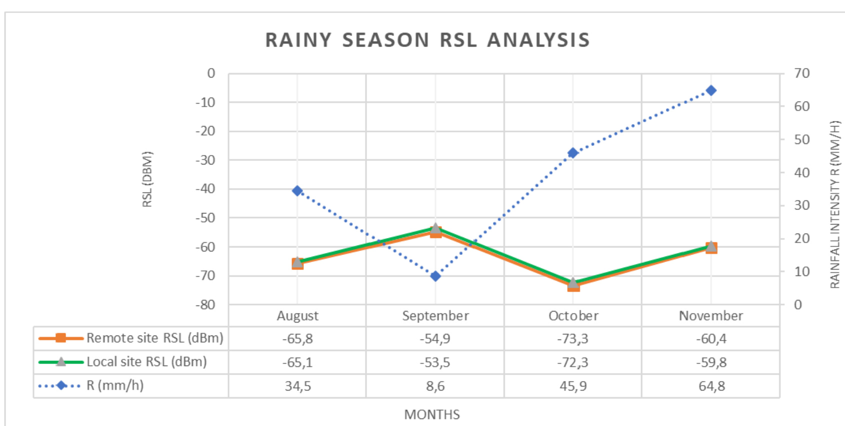

Figure 12. Rainy season Received Signal Level (RSL) analysis.

The ITU-R P.837 model is recommended for the dimensioning of traditional microwave links, operating at the limits of propagation conditions. However, the thresholds for weather phenomena must be more strict, up to 5 times those considered for traditional waves. This calls for the construction of a Rain Attenuation Model specific to millimeter waves in the coastal area of the Gulf of Guinea.

Our experimentation has confirmed the very high sensitivity of the millimeter wave to rain in line with the work of Weibel [26] and Sanyaolu [27].

4. CONCLUSION

The aim of our study was to contribute to the development of a prediction model that would enable more accurate design of millimeter transmission links in an equatorial climate environment such as the coastal zone of the Gulf of Guinea. To this end, we proposed a method for evaluating and measuring the propagation losses of an 80 GHz test link. This involved simulating the Evans and Friks models and the ITU-R P.837-7 model using Pathloss 5.1 microwave Design tool, which we previously calibrated based on data from ground and overground profile measurement surveys. The Nokia 80UBT test link was then installed at full scale and remotely monitored from the Nokia NFM-P platform. Using the environmental observatory deployed in the Tongo-Bassa watershed in the city of Douala (Cameroon), we were able to measure millimeter wave attenuation in free space and attenuation due to rainfall. The data collected from December 06, 2020 to December 16, 2021 led to a two-phase analysis: dry season and rainy season. The propagation of the millimeter signal in the Tongo-Bassa watershed located in the city of Douala, a part of the coastal area of the Guinea Gulf, follows the deterministic laws of Evans and Friks during the dry season. Our study confirms that the free space attenuation of the millimeter link remains within the ± 3 dB standard sizing margin approved by Orange Cameroon for microwave links. It can also be seen that the link is broken for rainfall intensities greater than 64.8 mm/h. This calls into question the ITU-R P.837-7 method, which estimates this break at a threshold of 110.1 mm/h. This study can be improved by measuring not only one link, but also a set of millimeter wave link installed in the same area. Indeed, the test link was designed for maximum performance: wide channel (1500 MHz), low cut-off margin (3.89 dB at 256 QAM modulation), and long distance (3.58 km). Also rainfall measurements were taken at ground level, while their impact on the link occurs 40 m from the ground where the antennas and ODU are installed. And beyond the rains, the effects of the wind and the expansion of the metal structures of the pylons were not integrated into our study.

ACKNOWLEDGMENT

We are very grateful to Dr. Marielle GOSSET from IRD/GET (Geosciences Environment Toulouse) who, since 2016, led an international team of scientists and made available the installation of the environmental observatory of the "Douala, Sustainable City: Sustainable development and valorization of the Makèpè Missokè site" in the Tongo-Bassa watershed. In fact, this work was carried out with the scientific, technical and financial support of the Interdisciplinary Research Program on Climate and Urban Environment (PRInCE), within the framework of the French Development Agency (FDA) and the Douala City Council (DCC) Convention. The mobile phone operator Orange Cameroon also made a strong contribution by authorising the collection, analysis and publication of data relating to the very first 80 GHz link ever installed in its network and on Cameroonian territory.

REFERENCES

1. Collonge, S., "Caractérisation et modélisation de la propagation des ondes électromagnétiques à 60 GHz à l'intérieur des bâtiments," *Diss. INSA de Rennes*, 2003.
2. Ericsson, A. B., "Delivering high-capacity and cost-efficient backhaul for broadband networks today and in the future," 2015.
3. ITU-R.2006, "Dispositions des canaux radioélectriques et des blocs de fréquences radioélectriques pour les systèmes hertziens fixes fonctionnant dans les bandes 71–76 et 81–86 GHz," International Telecommunication Union, Geneva, Switzerland, 2012.
4. Huawei, "Huawei RTN 300 *E-band Microwave*," 2016.
5. Ceríaco, L. M. P., B. S. Santos, R. F. Lima, et al., "Physical geography of the Gulf of Guinea oceanic islands," *Biodiversity of the Gulf of Guinea Oceanic Islands: Science and Conservation*, 13–36, Springer Cham, 2022, DOI https://doi.org/10.1007/978-3-031-06153-0.
6. Arato, S. S. and V. K. Oduol, "Performance analysis of E-band 70/80 GHz frequency segment for point to point gigabit connectivity," *International Journal for Innovation Education and Research*, Vol. 4, No. 4, 2016.

7. Ntanguen, P. H., A. N. Takougang, and A. T. Sandjon, "Raindrop size distribution and rainfall attenuation modeling from disdrometer measurement in Central Africa: Case of Cameroon," *Progress In Electromagnetics Research C*, Vol. 121, 243–253, 2022.
8. Tonye, E., "Développement des Télécommunications au Cameroun à l'horizon 2035," 2012, www.enspy-telecom.org.
9. Alhilali, M., J. Din, M. Schönhuber, and H. Y. Lam, "Estimation of millimeter wave attenuation due to rain using 2D video distrometer data in Malaysia," *Indonesian Journal of Electrical Engineering and Computer Science*, Vol. 7, No. 1, 164–169, 2017, DOI: 10.11591/ijeecs.v7.i1.
10. Mom, J., S. Soo Tyokighir, and G. Igwue, "Development of a new rain attenuation model for tropical location," *Indonesian Journal of Electrical Engineering and Computer Science*, Vol. 24, No. 2, 937–948, 2021, DOI: 10.11591/ijeecs.v24.i2.
11. Ghanim, M., M. Alhilali, J. Din, and H. Y. Lam, "Rain attenuation statistics over 5G millimetre wave links in malaysia," *Indonesian Journal of Electrical Engineering and Computer Science*, Vol. 14, No. 2, 1012–1017, 2019, DOI: 10.11591/ijeecs.v14.i2.
12. Evans, B., "Planning a microwave link: It's not just line of sight! Evans engineering solutions," *Broadcasters Clinic, Middleton, WI*, 2012.
13. Alcatel University, "Introduction aux Faisceaux Hertziens," 8AS 90001 1774 VT ZZB, 2008.
14. Lehpamer, H., "Microwave transmission networks: Planning, design, and deployment," McGraw-Hill Education, 2010.
15. Samad, Md A., F. D. Diba, and D.-Y. Choi, "A survey of rain attenuation prediction models for terrestrial links — Crrent research challenges and state-of-the-art," *Sensors*, Vol. 21, No. 4, 1207, 2021.
16. ITU, Recommandation UIT-R P.837-7, "Caractéristiques des précipitations pour la modélisation de la propagation," 2017.
17. ITU, Recommandation ITU-R P.838-3, "Specific attenuation model for rain for use in prediction methods," 2005.
18. Nauval, F., M. Marzuki, and H. Hashiguchi, "Regional and diurnal variations of rain attenuation obtained from measurement of raindrop size distribution over Indonesia at Ku, Ka and W bands," *Progress In Electromagnetics Research M*, Vol. 57, 25–34, 2017.
19. CUD, "Plan Directeur d'Urbanisme de Douala à l'horizon 2025," 2015.
20. Minepded, PNACC-Cameroun, "Plan National d'Adaptation aux Changements Climatiques du Cameroun," *Ministère de l'environnement, de la protection de la nature et du développement durable*, 2015.
21. Iroume, J. Y.-A., R. Onguéné, F. Djanna Koffi, A. Colmet-Daage, T. Stieglitz, W. Essoh Sone, S. Bogning, J. M. Olinga Olinga, R. Ntchantcho, J.-C. Ntonga, et al., "The 21st August 2020 Flood in Douala (Cameroon): A major urban flood investigated with 2D HEC-RAS modeling," *Water*, Vol. 14, 1768, 2022, https://doi.org/10.3390/w14111768.
22. Ntanguen, P. H., A. Nzeukou, R. Onguene, A. T. Sandjon, and R. Sonfack, "Parametrization of drop size distribution with rain rate for microwave and millimeter wave applications in Central Africa," *Indian J. Phys.*, 2023, https://doi.org/10.1007/s12648-023-02664-5.
23. Yves, R. H. and Associés Inc., "Pathloss 5.0 Training Course: Part II," Software Operation, Feb. 4, 2014.
24. Tanessong, R. S., D. A. Vondou, Z. Y. Djomou, et al., "WRF high resolution simulation of an extreme rainfall event over Douala (Cameroon): A case study," *Modeling Earth Systems and Environment*, Vol. 3, 927–942, 2017.
25. Findi, E. N., M. N. Wantim, and S. N. Ayonghe, "Assessing rainfall and temperature trend: Implication on flood patterns in vulnerable Communities of Limbe and Douala, Cameroon," *International Journal of Environmental Science*, Vol. 7, 2022.
26. Weibel, G. and H. Dressel, "Propagation studies in millimeter-wave link systems," *Proceedings of the IEEE*, Vol. 755, No. 4, 497–513, 1967.

27. Sanyaolu, D., O. F. Dairo, A. O. Soge, and A. A. Willoughby, "Prediction of rain-induced attenuation along earth-space links at millimeter wave bands over West African Region," *Telecommunications and Radio Engineering*, Vol. 80, No. 11, 2021.